Available online at www.sciencedirect.com
ScienceDirect
International Journal of Thermal Sciences 47 (2008) 1639–1646
International Journal of Thermal Sciences
www.elsevier.com/locate/ijts

A finite element model of solar heating system with underground storage

A. Ucar *, M. Inalli

Department of Mechanical Engineering, Firat University, 23279 Elazığ, Turkey

Received 24 April 2007; received in revised form 13 November 2007; accepted 9 December 2007

Available online 25 January 2008

Abstract

In this study, the performance of a solar heating system with seasonal storage is evaluated using finite element method. The time-dependent heat transfer problem between storage and the surrounding ground is solved by using a computer program in MATLAB and the transient temperature distribution in ground and transient temperature of water in the storage are calculated. The effects of storage volume and solar collector area on annual average temperature distribution in the ground surrounding storage are investigated. It is observed that the temperature of water in the storage increases with increase of the solar collector area. It was found that the water temperature for storage surrounded with sand ground was higher than the other ground types.

Keywords: Solar energy; Seasonal storage; Finite element

1. Introduction

The store of solar heat from the summer to the winter for space heating is important because of large differences between solar energy supply and heat demand. Solar collectors and storage are the most important economic parameters within these systems and most of the remaining costs can often be parameterized using these two components. The water temperature in under-ground storage must be known for the analysis and design of these energy systems. The various methods are used for solution of the transient heat transfer problem between storage and the surrounding ground in literature. Breger et al. [1] developed a comparative analysis of the heat transfer from boreholes and U-tubes using analytical solutions, finite element modeling and the available simulation model. This analysis is used to support the development of a methodology by which the heat transfer of any U-tube configuration can be modeled by appropriately specifying parameters in the borehole storage simulation model. Yumrutaş and Ünsal [2] obtained an analytical solution for the transient temperature field outside a hemispherical surface tank by an application of the Complex Finite Fourier Transform and the Finite Bessel Transform techniques. In this study, the effects of geological structure surrounding the tank, insulation thickness and tank size on the water temperature in the tank and also effect of tank size on the heat pump COP for different types of ground were investigated.

The transient temperature of water in the storage and the temperature distribution in surrounding ground must be known for the analysis of these systems. But, the solution of this temperature distribution problem is not easy. The finite element method, with its flexibility in dealing with complex geometries, is an ideal approach to employ in the solution of such problems. Therefore, the finite element method was used for solution of time-dependent heat transfer problem between storage and the surrounding ground in this study. A computer program in MATLAB was developed and used to determine the transient temperature distribution in ground and transient temperature of water in the storage. Analysis was performed for a solar heating system with seasonal storage located in Elazığ, Turkey. The load size considered was 1 housing unit with annual heat load of 87.6 MWh.

2. The thermal system

Schematic diagram of a central solar heating system with seasonal storage is shown in Fig. 1. The model system includes

* Corresponding author. Tel.: +90 0424 2370000/5333; fax: +90 424 2415526.
E-mail address: aucar@firat.edu.tr (A. Ucar).

1290-0729/$ – see front matter
doi:10.1016/j.ijthermalsci.2007.12.002

Nomenclature

A_c	Collector area ..... m^2	Q_u	Monthly average of useful solar energy ..... W
COP	The coefficient of performance of heat pump	T_a	Ambient temperature ..... K
D_1	Storage burial depth ..... m	T_{iref}	Inside design air temperature ..... K
F_R	Collector heat removal factor	T_f	Fluid temperature at the inlet to the collector ... K
I_T	Monthly average daily solar radiation incident on the collector per unit area ..... MJ/m^2	V_R	Average wind velocity ..... m/s
k	Thermal conductivity ..... W/m K	$(UA)_H$	Building loss coefficient ..... W/K
h	The convective heat transfer between air and ground ..... W/m^2 K	U_L	Collector overall energy loss coefficient W/m^2 K
Q_H	Heat load of building ..... W	W	Heat pump power
Q_{ie}	Net energy input rate to storage ..... W	ρ	Density ..... kg/m^3
		$(\tau\bar{\alpha})$	Average transmissivity absorptivity product

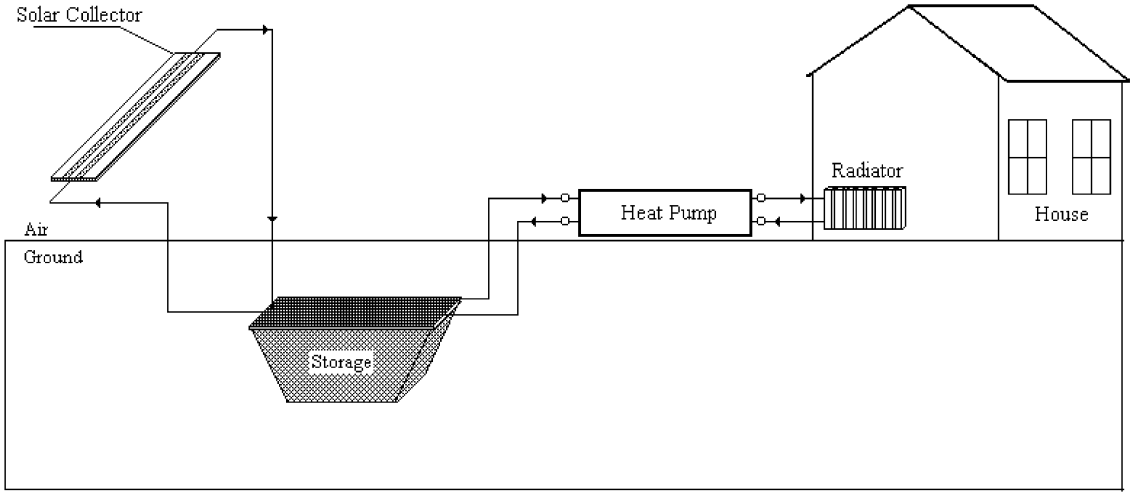

Fig. 1. Schematic diagram of a central solar heating system with seasonal storage.

flat plate solar collectors, a heat pump, an under ground storage tank and a heating load. Solar energy absorbed by the solar collectors is transferred to storage tank in the ground during the whole year. In the winter, the heat pump operates for heat supply, to extract the heat pump from the storage tank to the building. The heat pump operates only when the temperature of the water in the tank is in sufficient to keep the house at the required inside design air temperature. Therefore, the performance of a solar heating system with seasonal storage is directly related to the water temperature of the storage tank.

3. Numerical analysis

The transient heat transfer between storage and the surrounding ground is modeled by using a finite element model. An initial water temperature was assumed equal to the deep ground temperature which taken as 15 °C. The temperature beyond to depth of ground is taken as constant and equal to the deep-ground temperature. The ground surrounding the storage tank is assumed to have constant thermal conductivity. The initial temperature at the ground and storage is taken to be 15 °C, which is the deep ground temperature. The geometry of trapeze storage and the surrounding ground is developed as shown in Fig. 2.

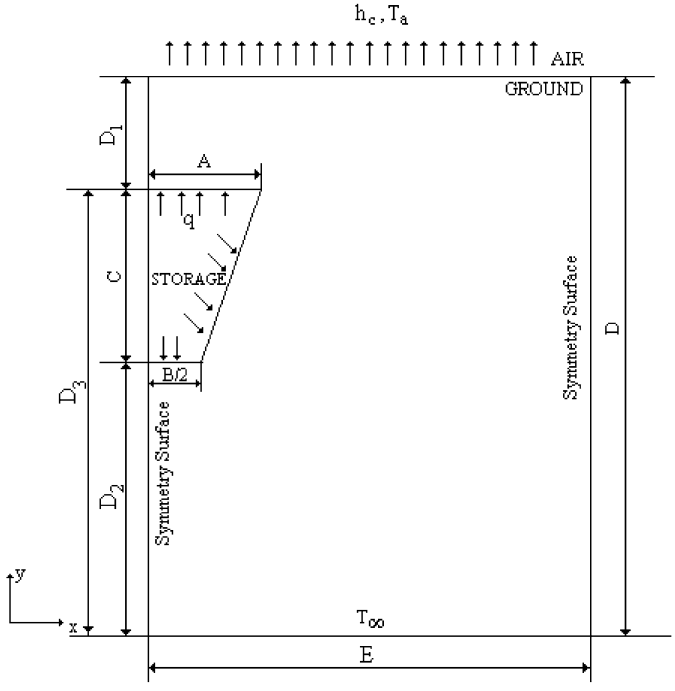

Fig. 2. The geometry of trapeze storage and the surrounding ground.

Q_{ie} is the net energy input rate to storage and evaluated as follows:

$$Q_{ie} = Q_u - Q_H + W \tag{1}$$

where Q_u is the useful energy gain of the flat plate collectors, Q_H is instantaneous heat load for building and W is heat pump work. Q_u and Q_H are calculated by

$$Q_u = A_c F_R\left[(\overline{\tau\alpha})I_T - U_L(T_f - T_a)\right] \tag{2}$$

$$Q_H = (UA)_H(T_{\text{iref}} - T_a) \tag{3}$$

where I_T is the instantaneous solar radiation incident on the collector per unit area, A_c is the collector area, F_R is the collector heat removal factor, $(\overline{\tau\alpha})$ is the transmittance, U_L is the collector overall loss coefficient, $(UA)_H$ is the heat loss coefficient of building, T_a is the ambient temperature. The coefficient of performance of heat pump is defined as

$$\text{COP} = \frac{Q_L}{W} \tag{4}$$

The Fourier's law of conductivity equation for heat transfer between storage and the surrounding ground is written below:

$$-\left(\frac{\partial q_x}{\partial x} + \frac{\partial q_y}{\partial y}\right) = \rho c \frac{\partial T}{\partial t} \tag{5}$$

The heat flux vectors for isotropic materials are given by

$$\vec{q}_x = -k\frac{\partial T}{\partial x} \tag{6}$$

$$\vec{q}_y = -k\frac{\partial T}{\partial y} \tag{7}$$

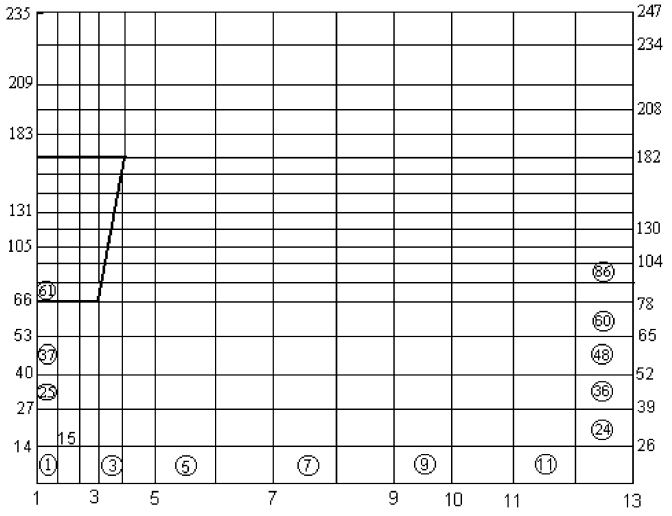

Fig. 3. The finite element model of the trapeze storage and surrounding ground.

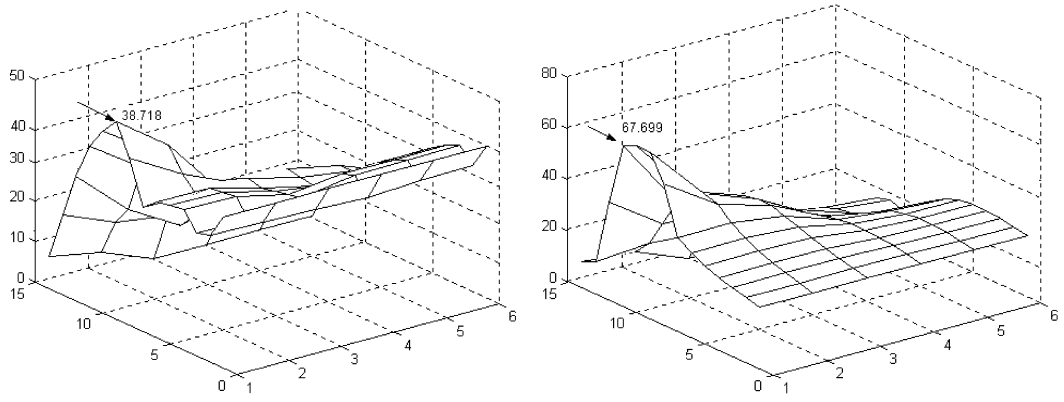

(a) 20 m^2 collector area (b) 30 m^2 collector area

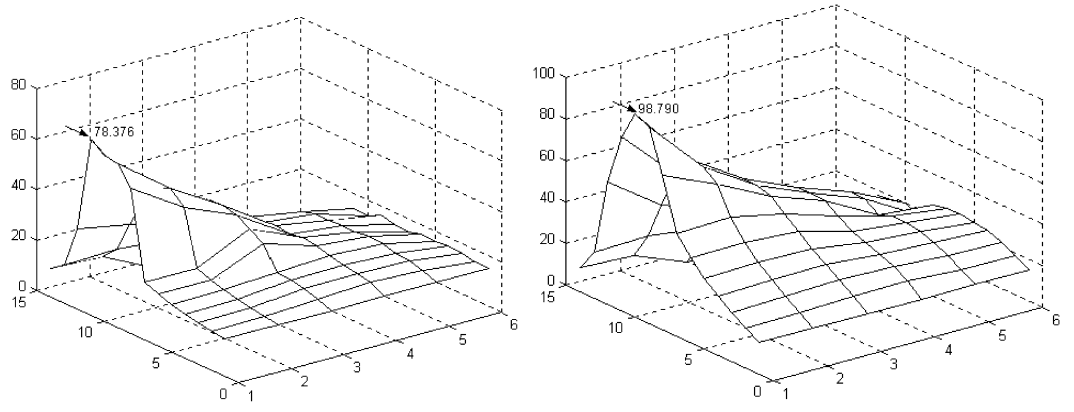

(c) 40 m^2 collector area (d) 50 m^2 collector area

Fig. 4. Effect of collector area on annual average temperature distribution in the ground surrounding storage (clay, $A = 14$ m, $B = 28$ m, $C = 28$ m, $D_1 = 10$ m).

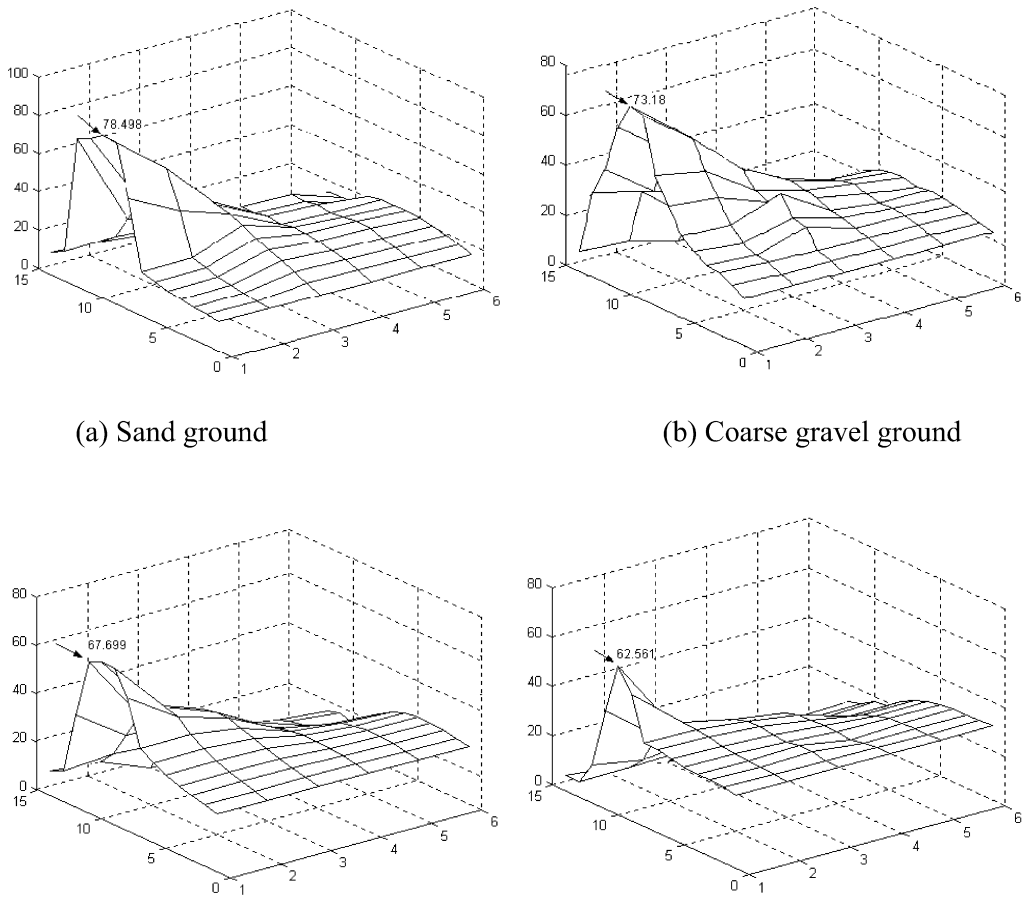

(a) Sand ground (b) Coarse gravel ground

(c) Clay ground (d) Granite ground

Fig. 5. Effect of ground type on annual average temperature distribution in the ground surrounding storage ($A_c = 30$ m^2, $A = 14$ m, $B = 28$ m, $C = 28$ m, $D_1 = 10$ m).

If Eq. (5) is written again for two-dimensional isotropic materials, it follows that

$$k\left(\frac{\partial^2 T}{\partial x^2} + \frac{\partial^2 T}{\partial y^2}\right) = \rho c \frac{\partial T}{\partial t} \tag{8}$$

The initial and boundary conditions are

$$T(x, y, 0) = T(x, y, \text{one year}) \tag{9a}$$

$$-k\frac{\partial T(x, y.t)}{\partial x} = h_c\big[T(x, y, t) - T_a\big] \quad \text{for } 0 < x < E \text{ and } y = D \tag{9b}$$

$$T(x, y, t) = T_\infty \quad \text{for } 0 < x < E \text{ and } y = 0 \tag{9c}$$

$$\frac{\partial T(x, y, t)}{\partial x} = 0 \quad \text{for } x = 0 \text{ and } 0 < y < D \tag{9d}$$

The convective heat transfer between air and ground is calculated using the following relation:

$$h_c = 5.7 + 3.8V_R \tag{10}$$

where V_R is average wind velocity and it is taken from the meteorological stations in Turkey. The temperature function for four-noded square element is given by [4]

$$T(x, y, t) = \sum_{i=1}^{r} N_i(x, y)T_i(t) = N_1T_1 + N_2T_2 + N_3T_3 + N_4T_4 \tag{11}$$

where N_1, N_2, N_3 and N_4 are element shape functions and these functions are evaluated by [3]

$$N_1 = \frac{1}{4}(1 - r)(1 - s) \tag{12}$$

$$N_2 = \frac{1}{4}(1 + r)(1 - s) \tag{13}$$

$$N_3 = \frac{1}{4}(1 - r)(1 + s) \tag{14}$$

$$N_4 = \frac{1}{4}(1 + r)(1 + s) \tag{15}$$

The isoparametric mapping is defined by

$$x = \frac{1}{4}\big[(1 - r)(1 - s)x_1 + (1 + r)(1 - s)x_2 + (1 + r)(1 + s)x_3 + (1 - r)(1 + s)x_4\big] \tag{16}$$

$$y = \frac{1}{4}\big[(1 - r)(1 - s)y_1 + (1 + r)(1 - s)y_2 + (1 + r)(1 + s)y_3 + (1 - r)(1 + s)y_4\big] \tag{17}$$

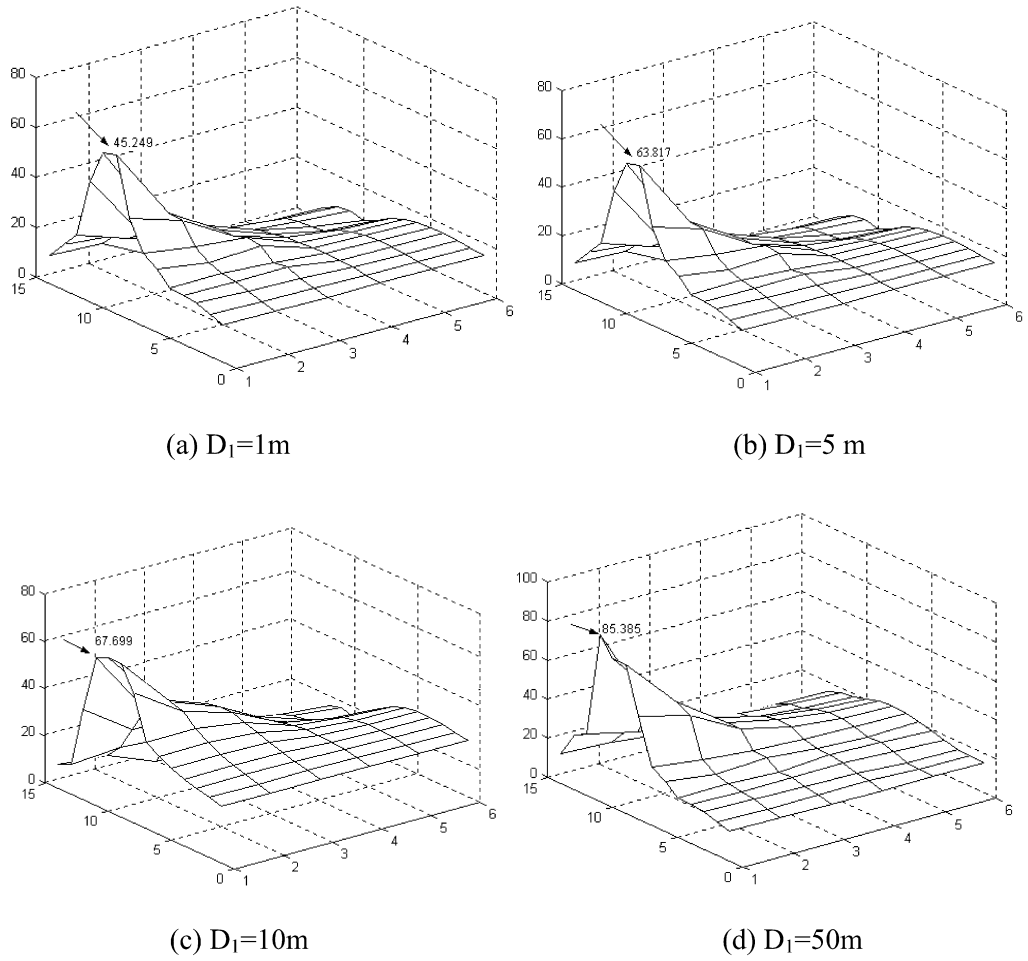

(a) D_1=1m (b) D_1=5 m

(c) D_1=10m (d) D_1=50m

Fig. 6. Effect of storage burial depths on annual average temperature distribution in the ground surrounding storage (clay ground, $A_c = 30\ \mathrm{m}^2$, $A = 14$ m, $B = 28$ m, $C = 28$ m).

For a general mapping transformation, an element of area $\mathrm{d}x\,\mathrm{d}y$ is transformed according to

$$\mathrm{d}x\,\mathrm{d}y = \det(J)\,\mathrm{d}r\,\mathrm{d}s \tag{18}$$

where J is the Jacobian matrix of the transformation which is defined by

$$J = \begin{bmatrix} \frac{\partial x}{\partial r} & \frac{\partial y}{\partial r} \\ \frac{\partial x}{\partial r} & \frac{\partial y}{\partial s} \end{bmatrix} \tag{19}$$

Applying the Galerkin approximate to Eq. (5), it follows that

$$\int_{\Omega^{(e)}} \left(\frac{\partial q_x}{\partial x} + \frac{\partial q_y}{\partial y} + \rho c \frac{\partial T}{\partial t} \right) N_i \,\mathrm{d}\Omega \tag{20}$$

where Ω is the solution domain. If we apply the Gauss theory to $\int_{\Omega^{(e)}} (\frac{\partial q_x}{\partial x} + \frac{\partial q_y}{\partial y}) N_i \,\mathrm{d}\Omega$, Eq. (20) can be expressed as

$$\int_{\Omega^{(e)}} \rho c \frac{\partial T}{\partial t} N_i \,\mathrm{d}\Omega - \int_{\Omega^{(e)}} \left| \frac{\partial N_i}{\partial x} \frac{\partial N_i}{\partial y} \right| \begin{Bmatrix} q_x \\ q_y \end{Bmatrix} \mathrm{d}\Omega = -\int_{\Gamma} N_i (q\tilde{n})\,\mathrm{d}\Gamma, \quad i = 1, 2, 3, 4 \tag{21}$$

Substituting the boundary conditions into Eq. (21) and it is expressed in the matrix form

$$|C| \frac{T_n - T_{n-1}}{\Delta t} + |K_C|\{T\} = \{R_T\} + \{R_q\} + \{R_h\} \tag{22}$$

where $|C|$ is the element matrix and $|K_C|$ is the element conduction matrix. $|C|$ and $|K_C|$ are obtained as:

$$|C| = \int_{\Omega} \rho c \{N\} |N| \,\mathrm{d}\Omega \tag{23}$$

$$|K_C| = \int_{\Omega^{(e)}} k |B|^T |B| \,\mathrm{d}\Omega \tag{24}$$

where $\{N\}$ is the temperature interpolation matrix. $|B|$ is defined by

$$|B| = \begin{vmatrix} \frac{\partial N_1}{\partial x} \frac{\partial N_2}{\partial x} \frac{\partial N_3}{\partial x} \frac{\partial N_4}{\partial x} \\ \frac{\partial N_1}{\partial y} \frac{\partial N_2}{\partial y} \frac{\partial N_3}{\partial y} \frac{\partial N_4}{\partial y} \end{vmatrix} \tag{25}$$

In Eq. (22), $\{R_q\}$ denotes the specified heat flux; $\{R_h\}$ denotes the surface convection and $\{R_T\}$ denotes the specified node temperature, defined as

$$\{R_q\} = \int_{S_1} q_S \{N\} \,\mathrm{d}\Gamma \tag{26}$$

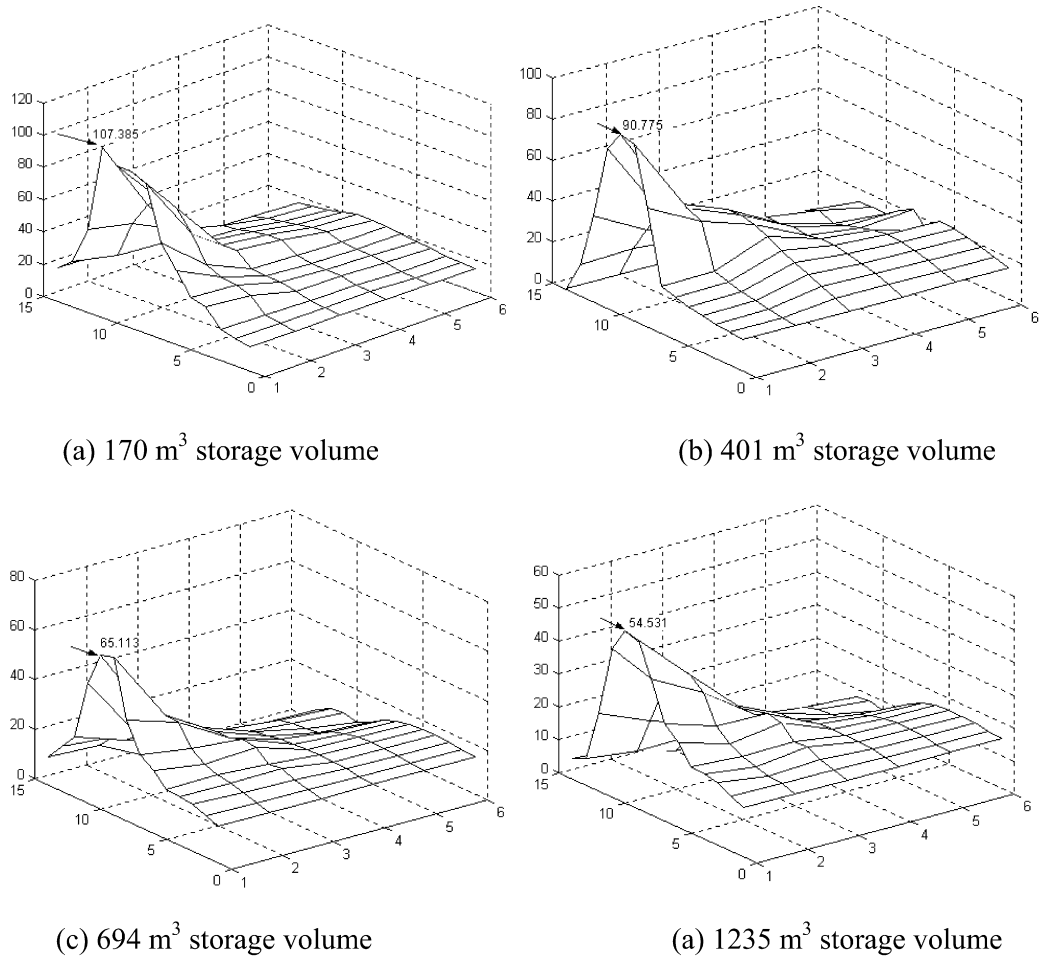

(a) 170 m^3 storage volume (b) 401 m^3 storage volume

(c) 694 m^3 storage volume (a) 1235 m^3 storage volume

Fig. 7. Effect of storage volume on annual average temperature distribution in the ground surrounding storage (clay ground, $A_c = 30$ m^2, $D_1 = 10$ m).

$$\{R_T\} = -\int_{S_2} (q\tilde{n})\{N\}\,\mathrm{d}\Gamma \tag{27}$$

$$\{R_q\} = \int_{S_3} hT_a\{N\}\,\mathrm{d}\Gamma \tag{28}$$

The accuracy of the numerical solution depends on the number of elements used. Actually, the number of elements used is determined by a compromise between the accuracy desired and the time required by the computer. The finite element mesh with 216 element and 247 nodes has been made in this study. The finite element model of the trapeze storage and surrounding ground is shown in Fig. 3. Because of the ground temperature faraway from the storage decreases, sizes of element field faraway the storage is increased. So, the time required by the computer is reduced.

4. Results of analysis and discussion

In this study, flat plate solar collector is used and collector parameters are $(\tau\alpha) = 0.76$, $U_L = 4.5$ W/m^2 K and $F_R = 0.95$. $(UA)_H$ value which is the ratio of the design heat load of the building to the winter design temperature difference is taken as 312.5 W/K. The data for the monthly average solar radiation on a horizontal surface and monthly average outside air temperature for Elazığ (38.7°N) were taken by the meteorological station in the Elazığ location of Turkey.

The thermal properties for the four different types of ground are given as: $\rho = 1500$ kg/m^3, $C_p = 848$ J/kg K, $k = 1.4$ W/m K for clay, $\rho = 2050$ kg/m^3, $C_p = 1842$ J/kg K, $k = 0.519$ W/m K for coarse gravel, $\rho = 2640$ kg/m^3, $C_p = 811$ J/kg K, $k = 3$ W/m K for granite, $\rho = 1500$ kg/m^3, $C_p = 800$ J/kg K, $k = 0.3$ W/m K for sand.

A computer program in MATLAB was developed for solution of Eq. (22). This program was used to determine the annual average temperature of water in the storage and temperature distribution in the ground surrounding storage. The results in this study are valid for the periodic operation case of the system.

Fig. 4 shows the effect of collector area on annual average temperature distribution in the clay ground surrounding storage. The temperature of water in the storage increases with increase of the solar collector area. It is obtained that the highest water temperature in the storage is 98 °C for 50 m^2 solar collector area and 38 °C for 20 m^2 the solar collector area. The highest water temperatures in storage for 30 m^2 and 40 m^2 solar collec-

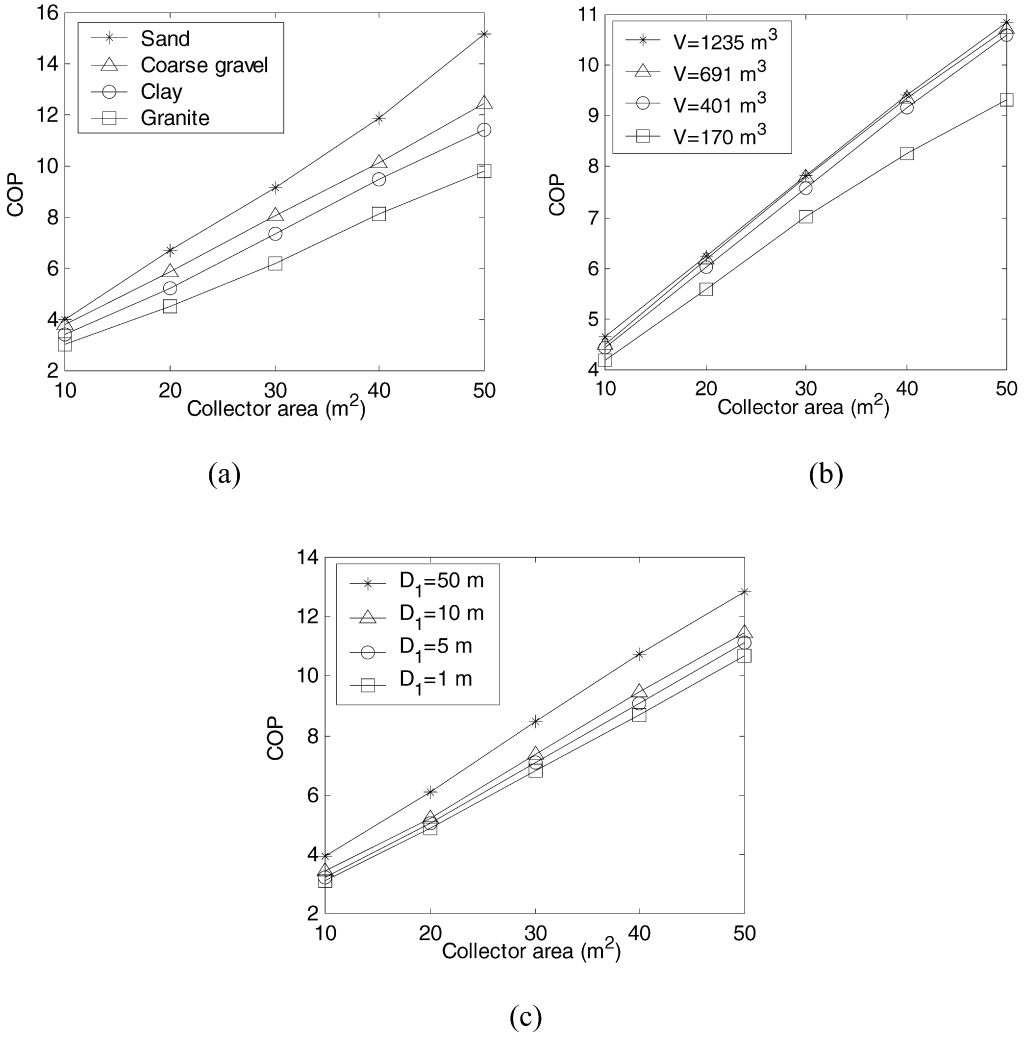

Fig. 8. Annual coefficient of performance of the heat pump as a function of collector area for (a) four different ground types, (b) for different storage volume, (c) for different storage burial depth.

tor areas are 31% and 20% lower than for 50 m^2 solar collector area, respectively.

The effect of ground type on annual average temperature distribution in the ground surrounding storage is depicted in Fig. 5. It is seen that the highest temperature is obtained when the storage is buried in sand ground. Heat absorbed by water in the storage will be transferred into surrounding ground since the ground having higher thermal conductivity and thermal diffusivity. The lowest water temperature takes place for the storage surrounded with granite ground having the highest thermal conductivity. It is observed that the highest temperature is 67.69 °C, i.e. 8% lower than for coarse gravel ground when storage is embedded in clay ground.

Fig. 6 shows the effect of storage burial depths on annual average temperature distribution in the ground surrounding storage. It is seen that the water temperature in storage increases with increase of the storage burial depth. The effect of ambient temperature on the water temperature in storage decreases with increase of the burial depth and therefore the water temperature in storage is higher when storage burial depth is 50 m. The water temperature in the storage embedded 1 meter below the ground surface is 47% lower than for 50 m storage burial depth.

The effect of storage volume on annual average temperature distribution in the ground surrounding storage is illustrated in Fig. 7. It is observed that the water temperature in the storage decreases with increase of the storage volume. The lowest temperature is obtained for the system with 1235 m^3 storage volume, while the highest water temperature occurs for the storage with 170 m^3 volume.

Fig. 8 illustrates the annual coefficient of performance (COP) of the heat pump as a function of collector area for four different ground types, for different storage volume, for different storage burial depth. Fig. 8(a) shows that the lowest COP is obtained when the storage is buried in granite. However, the highest COP is obtained for sand. It is observed that the COP increases with increase of the collector area. Fig. 8(b) shows that the highest COP is obtained for highest storage volume. In this figure, it is seen that the effect of storage volume on COP of heat pump decreases when the storage volume become suffi-

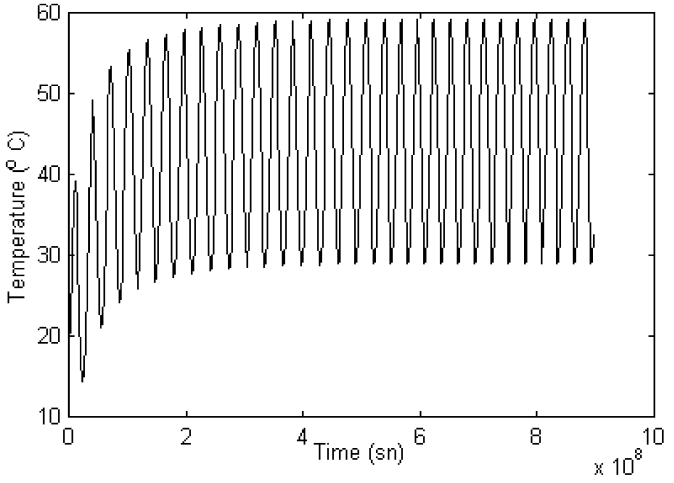

Fig. 9. Storage temperature variation through the simulation (granite ground, $A_c = 30\ \mathrm{m}^2$, $D_1 = 10\ \mathrm{m}$).

ciently large. The effect of storage burial depths on COP of heat pump is shown in Fig. 8(c). It is seen from this figure that the COP increases with increase of the storage burial depth. The lowest COP is obtained for the smaller burial depth.

The water temperature variation in the storage tank during years is given in Fig. 9. In order to reach the periodic operation regime, the system with storage embedded into granite ground needs approximately 15 years. It can be seen that the effect of ground on the long-term performance of the system importantly decreases after 15 years.

5. Conclusion

In this study, a solar heating system with seasonal storage buried inside ground is analyzed using finite element method. Finite element formulation of the transient heat transfer between trapeze storage and the surrounding ground is solved and the temperature distribution in ground is obtained. It is found that the water temperature in the storage increases with increase of solar collector area while the temperature decreases with increase of storage volume. The thermal performance of system with storage surrounded with sand ground having the lowest thermal conductivity is higher, compared with the other systems. It is seen from the results of this study that the water temperature in storage increases with increase of the storage burial depth. To obtain more effective performance, a solar heating system with seasonal storage can be designed using the information presented in this study.

References

[1] S.D. Breger, J.E. Hubbell, H.E. Hasnaoui, J.E. Sunderland, Thermal energy storage in the ground: comparative analysis of heat transfer modeling using u-tubes and boreholes, Solar Energy 56 (1996) 49–503.

[2] R. Yumrutaş, M. Ünsal, A computational model of a heat pump system with a hemispherical surface tank as the ground heat source, Energy 25 (2000) 371–388.

[3] G.A. Quadir, A. Mydin, K.N. Seetharannı, Analysis of microchannel heat exchangers using FEM, Int. J. Numer. Methods Heat Fluid Flow 11 (2001) 1–18.

[4] R.W. Lewis, K. Morgan, H.R. Thomas, K.N. Seetharamu, The Finite Element Method in Heat Transfer Analysis, John Wiley & Sons, 1996.